Dominant biaxial quadrupolar contribution to the nematic potential of mean torque

Fulvio Bisi
Dipartimento di Matematica and CNISM, Università di Pavia, Via Ferrata 1, 27100 Pavia, Italy

Geoffrey R. Luckhurst
School of Chemistry, University of Southampton, University Road, Southampton SO17 1BJ, United Kingdom

Epifanio G. Virga
Dipartimento di Matematica and CNISM, Università di Pavia, Via Ferrata 1, 27100 Pavia, Italy

(Received 28 February 2008; published 26 August 2008)

Within the general quadrupolar model for biaxial nematic liquid crystals, whose potential of mean torque extends that in the Maier-Saupe theory with two extra interaction terms, we propose a quantitative criterion to identify the dominant biaxial interaction. We show that the ratio of the biaxial-to-uniaxial and uniaxial-to-isotropic transition temperatures is almost independent of one interaction parameter, thus indicating the other as dominant. We also show that there is a significant mismatch between the principal orientational order parameters predicted by the theory and those measured for the biaxial phase of a tetrapode.

DOI: 10.1103/PhysRevE.78.021710 PACS number(s): 61.30.Cz, 61.30.Dk

I. INTRODUCTION

The thermotropic biaxial nematic phase, whose existence was predicted by Freiser in 1970 [1,2], promises to possess novel and applicable properties [3,4]. There has, therefore, been considerable interest in the creation of compounds which might exhibit the biaxial phase. However, it seems that many of the early claims to have found the biaxial nematic are false [5]. In relatively recent years there have been further claims to have discovered a biaxial nematic phase, for V-shaped molecules [6,7] and for tetrapode molecules in which four mesogenic groups are tethered laterally to a single silicon atom [8,9] and to a single germanium atom [10].

The evidence for these new claims seems to be stronger; indeed, somewhat surprisingly, it has proved possible to prepare a monodomain of the biaxial nematic phase thought to be exhibited by a tetrapode [8]. This has then been employed to determine the second-rank orientational order parameters in the biaxial nematic as well as the uniaxial nematic phase by using infrared spectroscopy. The four relevant order parameters are defined as [11–13]

$$S := S_{zz}^{ZZ}, \tag{1a}$$

$$D := S_{xx}^{ZZ} - S_{yy}^{ZZ}, \tag{1b}$$

$$P := S_{zz}^{XX} - S_{zz}^{YY}, \tag{1c}$$

$$C := (S_{xx}^{XX} - S_{yy}^{XX}) - (S_{xx}^{YY} - S_{yy}^{YY}), \tag{1d}$$

in terms of the entries of the *supermatrix* $\boldsymbol{S}$, where the superscript uppercase letters denote the principal laboratory axes and the subscript lowercase letters the principal molecular axes. The order parameters S and D are nonzero in the uniaxial nematic phase, whereas P and C are zero; in the biaxial nematic phase, all four order parameters S, D, P, and C are nonzero. In addition to the same S as in Eq. (1a), three other scalar order parameters—namely, S', T, and T'—were introduced in [14]; they are related to those in Eqs. (1b)–(1d) through the equations

$$S' = D, \quad T = \frac{1}{3}P, \quad T' = \frac{1}{3}C.$$

A fairly complete list of notation employed over the years in this field by different authors is given in [15] along with a convenient conversion table.[1] Individual molecules are assumed to possess D_{2h} symmetry, and their interaction is given the general quadrupolar expression put forward by Straley [16].

The heart of the molecular-field theory[2] is the potential of mean torque experienced by a molecule as a result of its anisotropic interactions with its neighbors. The potential of mean torque is restricted to second rank—that is, to quadrupolar terms—and takes the form [14,17–20]

$$U = -u_0\{\mathbf{q}\cdot\mathbf{Q} + \gamma(\mathbf{q}\cdot\mathbf{B} + \mathbf{b}\cdot\mathbf{Q}) + \lambda\mathbf{b}\cdot\mathbf{B}\}, \tag{2}$$

where the molecular orientation with respect to the directors is given by the two traceless, orthogonal tensors

[1]The scalar order parameters collected and classified in [15] are all quadrupolar in nature—that is, associated with a second-rank order tensor. All ordered phases formed by biaxial molecules are characterized by at most four such second-rank scalar order parameters. Clearly, a more accurate description could be gained by also calling upon scalar order parameters of higher rank. For example, this attitude was recently taken in [29] for the possible biaxial phases of uniaxial molecules, for which second- and fourth-rank scalar order parameters together add up to five, although, in general, there are four second-rank and nine fourth-rank scalar order parameters.

[2]The term *molecular field* is used here to distinguish theories such as that of Maier and Saupe for nematics which have a clear molecular basis from *mean-field* or Landau theories which involve phenomenological expansions of scalar invariants of the relevant order tensors characterizing the phases.

$$\mathbf{q} := \boldsymbol{e}_z \otimes \boldsymbol{e}_z - \frac{1}{3}\mathbf{I}, \quad \mathbf{b} := \boldsymbol{e}_x \otimes \boldsymbol{e}_x - \boldsymbol{e}_y \otimes \boldsymbol{e}_y.$$

Here $\mathbf{I}$ is the identity tensor and $\{\boldsymbol{e}_x, \boldsymbol{e}_y, \boldsymbol{e}_z\}$ are orthonormal unit vectors parallel to the molecular symmetry axes. The tensors $\mathbf{Q}$ and $\mathbf{B}$ in Eq. (2) are related to the orientational order parameters by

$$\mathbf{Q} = S\left(\boldsymbol{e}_Z \otimes \boldsymbol{e}_Z - \frac{1}{3}\mathbf{I}\right) + \frac{1}{3}P(\boldsymbol{e}_X \otimes \boldsymbol{e}_X - \boldsymbol{e}_Y \otimes \boldsymbol{e}_Y),$$

$$\mathbf{B} = D\left(\boldsymbol{e}_Z \otimes \boldsymbol{e}_Z - \frac{1}{3}\mathbf{I}\right) + \frac{1}{3}C(\boldsymbol{e}_X \otimes \boldsymbol{e}_X - \boldsymbol{e}_Y \otimes \boldsymbol{e}_Y),$$

where $\{\boldsymbol{e}_X, \boldsymbol{e}_Y, \boldsymbol{e}_Z\}$ is the laboratory eigenframe shared by both tensors. The potential U in Eq. (2) clearly appears as an extension of that in the Maier-Saupe theory [21] through the addition of the terms in γ and λ. It is a major purpose of this paper to show that the latter is indeed the dominant term according to a criterion that we develop below. Our other important aim is to compare the predicted order parameters with those measured for a tetrapode [8].

The paper is organized as follows. In Sec. II, we show by which criterion the biaxial contribution in λ to the potential of mean torque in Eq. (2) can indeed be considered as dominant. Our dominance criterion will also suggest a natural way to compare our mathematical model with experiment; such a comparison is presented in Sec. III. Finally, in Sec. IV we summarize our work and comment on the outcomes of our comparison with experiment.

II. DOMINANT CONTRIBUTION

In the potential of mean torque in Eq. (2), the positive parameter u_0 is related to the molecular anisotropy and is used to scale the absolute temperature T. The relative molecular biaxiality is related to both γ and λ, the model parameters of the theory, subject to the inequalities

$$\lambda > 0, \quad 1 - |2\gamma| + \lambda > 0, \tag{3}$$

which ensure the stability of the ground state where the interacting molecules lie parallel to one another. However, not all points in the fan-shaped region of the (γ,λ) plane defined by Eqs. (3) correspond to physically distinguished molecular states: by properly exchanging the roles of the molecular axes [20,22], all inequivalent states can be represented by points within the *essential triangle* with vertices at the points $\mathsf{O}=(0,0)$, $\mathsf{I}=(0,\frac{1}{3})$, and $\mathsf{V}=(\frac{1}{2},0)$ of the (γ,λ) plane (see Fig. 1). Similar symmetry transformations apply to the scalar order parameters (S,D,P,C), so that multiple representations are possible for one and the same condensed phase [20]. Here we adopt the representation in which a uniaxial state possesses $S>D>0$ and $P=C=0$, which is the usual choice in describing experimental data.

The theory, already presented in [14,19,20,23], builds the molecular-field free energy F from the potential of mean torque, U:

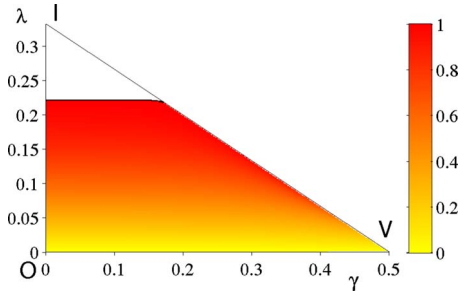

FIG. 1. (Color online) The essential triangle OVI in the (γ,λ) plane with a pseudocolor map of the ratio $\rho := T_{N_B\text{-}N_U}/T_{N_U\text{-}I}$ between the biaxial-to-uniaxial and uniaxial-to-isotropic transition temperatures. A colorbar is added on the right side of the graph to illustrate the scale. The triple line is the upper (red) line bounding the colored region. When $\rho \simeq 1$ the two transition temperatures are close to one another and the corresponding points are, therefore, close to the triple line where $\rho=1$; when $\rho \simeq 0$, the biaxial-to-uniaxial transition tends to disappear and the corresponding points are close to the base OV of the essential triangle.

$$F = \frac{u_0}{3}\left\{S^2 + \frac{1}{3}P^2 + 2\gamma\left(SD + \frac{1}{3}PC\right) + \lambda\left(D^2 + \frac{1}{3}C^2\right) - \frac{3}{\beta}\ln\left(\frac{Z}{8\pi^2}\right)\right\}, \tag{4}$$

where

$$Z := \int_0^{2\pi} d\psi \int_0^{2\pi} d\varphi \int_0^{\pi} d\vartheta \sin\vartheta \exp(\beta g) \tag{5}$$

is the partition function. The molecular orientation with respect to the laboratory frame $\{\boldsymbol{e}_X, \boldsymbol{e}_Y, \boldsymbol{e}_Z\}$ is described by the Euler angles (ϑ,φ,ψ) in the y notation [15]. In Eq. (5), $\beta := u_0/k_BT$, k_B is the Boltzmann constant and

$$\begin{aligned} g &:= \mathbf{q}\cdot\mathbf{Q} + \gamma(\mathbf{q}\cdot\mathbf{B} + \mathbf{b}\cdot\mathbf{Q}) + \lambda\mathbf{b}\cdot\mathbf{B} \\ &= \left(\cos^2\vartheta - \frac{1}{3}\right)(S + \gamma D) \\ &\quad + \sin^2\vartheta\left[\frac{1}{3}(P + \gamma C)\cos 2\varphi + (\gamma S + \lambda D)\cos 2\psi\right] \\ &\quad + \frac{1}{3}[(1 + \cos^2\vartheta)\cos 2\varphi\cos 2\psi - 2\cos\vartheta\sin 2\varphi\sin 2\psi] \\ &\quad \times(\gamma P + \lambda C). \end{aligned}$$

To obtain the order parameter profiles for a choice of γ and λ, we perform a bifurcation analysis of the equilibrium equations for F with the aid of MATCONT [24], a free software package which is integrated into MATLAB [25]. In our parametrization, the equilibrium equations for F, yielding the states compatible with the molecular field, read as

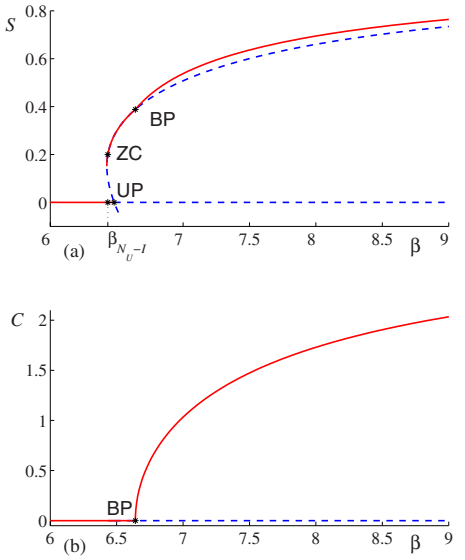

FIG. 2. (Color online) Bifurcation diagrams for $\gamma=\gamma_A=0.174$ and $\lambda=\lambda_A=0.193$, corresponding to the point in the (γ,λ) plane designated by a star in Fig. 3. Solid (red) lines represent stable equilibria. Dashed (blue) lines represent unstable equilibria. (a) S against β. UP is the point where an unstable uniaxial branch bifurcates from the isotropic line. ZC is the point where the free energy of the stable uniaxial equilibrium is equal to zero—that is, to the free energy of the isotropic state. The point ZC occurs at $\beta=\beta_{N_U\text{-}I}=6.43$. BP is the point on the uniaxial branch where a biaxial branch bifurcates with exchange of stability. The primary, uniaxial-to-isotropic transition is first order, whereas the secondary, biaxial-to-uniaxial transition is second order. (b) C against β. These branches illustrate the same solutions as in (a). The BP points in the two bifurcation diagrams correspond to one another; they occur at one and the same value of β, $\beta_{N_B\text{-}N_U}=6.64$.

$$\frac{2}{3}(S+\gamma D)-\frac{Z_S}{Z}=0,\quad \frac{2}{3}(\gamma S+\lambda D)-\frac{Z_D}{Z}=0,$$

$$\frac{2}{3}(P+\gamma C)-\frac{Z_P}{Z}=0,\quad \frac{2}{3}(\gamma P+\lambda C)-\frac{Z_C}{Z}=0,$$

where Z_X denotes the partial derivative of Z with respect to the corresponding order parameter, X.

In the numerical bifurcation analysis, a continuation in the parameter β is started from the isotropic state, characterized by the vanishing of all order parameters (see Fig. 2). By using MATCONT with a specifically designed code, we identify a bifurcation point on the isotropic branch; we label this point UP: it is the point where the isotropic solution loses its stability. A second equilibrium solution branches off from UP at $\beta=\beta_{\mathrm{UP}}$; this solution branch has nonzero S (and, correspondingly, nonzero D), but $P=C=0$: it describes nematic uniaxial states. In general, moving along the uniaxial branch one first encounters unstable equilibrium points and then stable ones. By monitoring the free energy of the stable states, we identify the transition value $\beta=\beta_{N_U\text{-}I}$, yielding $T_{N_U\text{-}I}$: the transition is marked by the free energy of the nematic uniaxial state crossing zero, the value for the isotropic phase according to Eq. (4). We label this point on the bifurcation graph as ZC. On the uniaxial branch, stability is then lost at a second bifurcation point, labeled as BP, from which a solution branches off with all four order parameters different from zero. This is a biaxial nematic branch, and a transition onto it from the uniaxial branch occurs when the free energy is equal on the two branches: this is the condition identifying the value $\beta=\beta_{N_B\text{-}N_U}$, which yields $T_{N_B\text{-}N_U}$. While the uniaxial-to-isotropic (N_U-I) transition is always first order, the biaxial-to-uniaxial (N_B-N_U) transition can be either first or second order, depending on the profile of the bifurcating biaxial branch. Thus, the N_B-N_U transition line in the phase diagram may bear a tricritical point [17,19,20,23,26]. Correspondingly, a *tricritical line* can be drawn in the essential triangle, which divides it into two regions, according to whether the secondary biaxial-to-uniaxial transition is first or second order (see Fig. 3). Moreover, a *triple line* can be drawn corresponding to the points where the isotropic, uniaxial, and biaxial phases are in equilibrium (see Figs. 1 and 3): above the triple line, a direct transition occurs be-

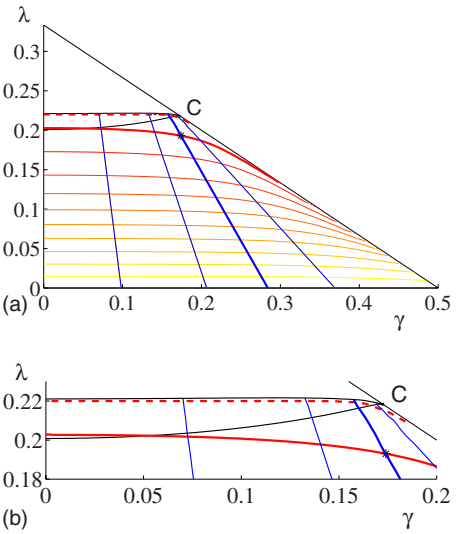

FIG. 3. (Color online) (a) Contour map of the ratio $\rho:=T_{N_B\text{-}N_U}/T_{N_U\text{-}I}$ between the biaxial-to-uniaxial and uniaxial-to-isotropic temperatures as a function of the parameters (γ,λ) in the potential of mean torque in Eq. (2), restricted to the essential triangle. The solid lines meeting at the point C on the oblique side of the essential triangle are the triple (above) and the tricritical (below) black lines. The thin lines correspond to values of ρ equally spaced between 0.1 and 0.9. The thick lines correspond to the tetrapodes A (solid line, $\rho_A=0.969$) and B and C (dashed line, $\rho_B=\rho_C=0.999$). The isoratio line for tetrapodes B and C is hardly distinguishable from the triple line. The isoratio lines are traversed by the lines with equal $S_{N_U\text{-}I}$, the value of S at the N_U-I transition, here chosen as 0.4, 0.3, 0.2, and 0.1 (from left to right). The curves with equal $S_{N_U\text{-}I}$ are defined up to the triple line, as there the intermediate uniaxial phase ceases to exist. A star marks the point $(\gamma_A,\lambda_A)=(0.174,0.193)$ on the isoratio line for tetrapode A; with this choice of parameters in the potential of mean torque in Eq. (2), $S_{N_U\text{-}I}$ matches the value measured experimentally. The color code for the thin contour lines is the same as in Fig. 1. (b) Magnification of (a). The isoratio line for tetrapode A is mostly below the tricritical line, whereas the isoratio line for tetrapodes B and C is mostly above the tricritical line.

tween the isotropic and biaxial phases. For $\gamma=0$, the tricritical and triple lines are separate, but they merge in a point C on the IV side of the essential triangle [20] (see Fig. 3).

The quantitative criterion we propose to judge the relative importance of the two biaxial terms in the potential of mean torque in Eq. (2) is computing the ratio $\rho := T_{N_B\text{-}N_U}/T_{N_U\text{-}I} = \beta_{N_U\text{-}I}/\beta_{N_B\text{-}N_U}$, which, being independent of u_0, is only a function of (γ,λ) within the essential triangle in Fig. 1. Since only the direct biaxial-to-isotropic transition occurs on and above the triple line and along the IV side, ρ is not defined there. Similarly, only the uniaxial-to-isotropic transition occurs on the base OV, and so ρ is equally undefined there [19]. In Fig. 1, a pseudocolor map of ρ is reported in the essential triangle; the color code, illustrated by the colorbar, ranges from yellow for $\rho=0$ to red for $\rho=1$.

It is remarkable that ρ is so weakly dependent on γ, while it exhibits a strong dependence on λ. Figure 1 makes it visually evident that setting $\gamma=0$ in Eq. (2) would not appreciably affect the ratio ρ between the transition temperatures, though it affects some other properties of the condensed phases, such as the rebound of the uniaxial scalar order parameter D at the biaxial nematic transition studied in [23]. This indirectly supports the choice made in [27] of basing a Landau theory for biaxial nematic liquid crystals upon the potential with $\gamma=0$.

III. COMPARISON WITH EXPERIMENT

The independence of ρ upon u_0 also makes it a parameter of choice for comparing theory with experiment.

To this end, in Fig. 3 we build the contour plot of ρ, drawing the *isoratio* lines for equally spaced values of ρ in the range [0.1, 0.9]. In general, every isoratio line hits the segment CV on the IV side of the essential triangle in a different point, making it possibile to extend by continuity the definition of ρ up to the triple line, CV, and OV. In particular, $\rho\to 1$ on approaching the triple line and $\rho\to 0$ on approaching the base OV.

We shall focus attention on the isoratio lines corresponding to compounds that in the literature have been claimed capable of exhibiting thermally driven biaxial-to-uniaxial transitions. A specific experimental value of ρ allows us to select a single isoratio line, which thus identifies all possible values of (γ,λ) in Eq. (2) compatible with the measured transition temperature ratio. In particular, the data for tetrapode A of [8] show a first-order N_U-I transition at the temperature $T_{N_U\text{-}I}=320$ K and a second-order N_B-N_U transition at the temperature $T_{N_B\text{-}N_U}=310$ K. We take $T_{N_B\text{-}N_U}$ to be the temperature at which either P or C first becomes strictly nonzero, within experimental error. Accordingly, in Fig. 3 we report the curves for the two organosiloxane tetrapodes (A and B) explored in [8], as well as for the similar germanium compound studied in [10] (tetrapode C). Infrared spectroscopy measurements indicate for tetrapode A a ratio $\rho_A=0.969$, with a second-order N_B-N_U transition, and for tetrapode B a ratio $\rho_B=0.999$, with a weakly first-order N_B-N_U transition. Similarly, dynamic light-scattering measurements performed on a sample of tetrapode C yield $\rho_C=\rho_B$, also revealing a weakly first-order N_B-N_U transition. As can be seen from Fig. 3(b), both the corresponding isoratio lines cross the tricritical line, and so each of them would be compatible with either a first- or a second-order N_B-N_U transition, though the isoratio line corresponding to ρ_A is mostly below the tricritical line, whereas the isoratio line corresponding to $\rho_B=\rho_C$ is mostly above the tricritical line, which makes the biaxial-to-uniaxial transition more likely to be second-order for tetrapode A and first-order for tetrapodes B and C.

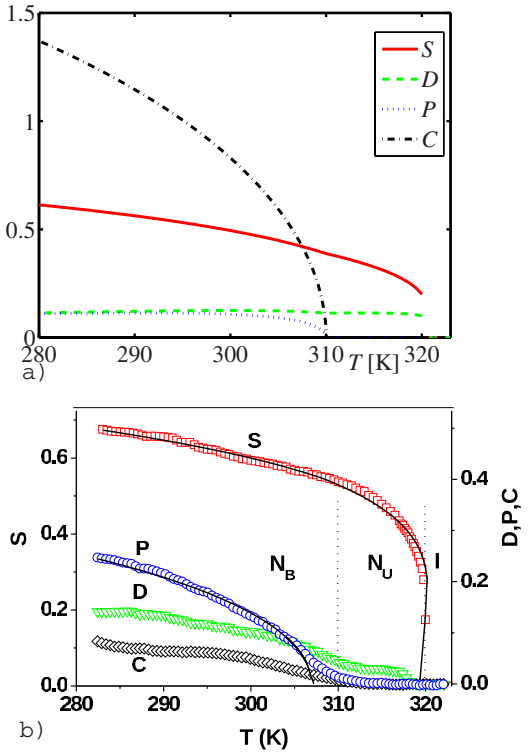

FIG. 4. (Color online) (a) Plots of the order parameters (S,D,P,C) against the absolute temperature T for $\gamma=0.174$ and $\lambda=0.193$. Color code: S (red), D (green), P (blue), and C (black). (b) Measured order parameters as shown in Fig. 3 of [8].

Only by using extra experimental data can we single out a point (γ_0,λ_0) on the isoratio line that describes a specific compound. In particular, the value $S_{N_U\text{-}I}$ of the primary order parameter S at the onset of the uniaxial phase for $T=T_{N_U\text{-}I}$ proved especially fit for this purpose. The lines with equal $S_{N_U\text{-}I}$ are superimposed onto the isoratio lines in Fig. 3 in the region of the essential triangle below the triple line, where they are both defined. These families of lines determine a grid capable of mapping unambiguously pairs $(\rho,S_{N_U\text{-}I})$ and (γ,λ) into one another. Thus, when an isoratio line ρ crosses the tricritical line, the knowledge of $S_{N_U\text{-}I}$ can decide whether for a specific compound the theory predicts the secondary N_B-N_U transition to be first or second order. For example, for tetrapode A we can read off from Fig. 3 of [8] that $S_{N_U\text{-}I} \simeq 0.20$; the corresponding point $(\gamma_A,\lambda_A)=(0.174,0.193)$ is marked in Fig. 3 with a star; it lies below the tricritical line, and so the N_B-N_U transition is predicted to be second order, as actually observed.

For $\gamma=\gamma_A$ and $\lambda=\lambda_A$, u_0 can be determined from either $\beta_{N_U\text{-}I}$ or $\beta_{N_B\text{-}N_U}$, since both $T_{N_U\text{-}I}$ and $T_{N_B\text{-}N_U}$ are known. Figure 4(a) shows the equilibrium order parameters (S,D,P,C)

predicted by theory as functions of the absolute temperature T; for comparison, we show in Fig. 4(b) their experimental counterparts measured for tetrapode A [8].

In the uniaxial nematic phase there is reasonably good agreement between the predicted and measured values of the nonzero order parameters S and D. Thus, in both cases the profiles for the major order parameter S are comparable in magnitude and have the same strong temperature dependence. Similarly, D, the molecular biaxial order parameter, is observed and predicted to be small as well as essentially independent of temperature. Within the biaxial nematic phase the major order parameter S continues to grow with decreasing temperature as predicted by the theory. In contrast, however, the observed behavior of the remaining order parameters D, P, and C deviates to different extents from that predicted. The most striking of these is found for the major biaxial order parameter C. Below about 308 K this is predicted to be the largest of the order parameters, but for the tetrapode it is the smallest. Indeed at the lowest temperature for which measurements are available its value is only about 0.09, whereas the predicted value at the same temperature is 1.4. The behavior of the other biaxial order parameter P also deviates, but less dramatically, from that predicted. Thus experimentally P grows continuously from zero at the N_B-N_U transition to about 0.25 at the lowest temperature. The predicted behavior is different, with a weak temperature dependence and a value at the lowest temperature of just 0.11. The deviation of the experimental behavior of the order parameter D from that given by theory is relatively minor. Thus it is predicted to decrease very slightly with decreasing temperature in the biaxial nematic phase and to have a value of about 0.11. Experimentally D is observed to increase more rapidly with decreasing temperature and to reach a value of 0.13 at the lowest temperature. However, we should note that careful examination of the predicted behavior of D does reveal a slight increase on entering the biaxial nematic phase, but this is far smaller than the increase shown by the experimental data. In summary, the behavior of S in both nematic phases is in good agreement with theory and so, to a lesser extent, is that of D. In contrast C is observed to be significantly smaller than predicted, while the behavior of P deviates, but to a lesser extent, from the theoretical predictions.

That among the biaxial scalar order parameters C always prevails over P we have no formal proof as yet. A numerical exploration has been performed for all points (γ,λ) coincident with the nodes of the grid determined below the triple line in the essential triangle of Fig. 3 by the isoratio lines and the lines with equal $S_{N_U\text{-}I}$. For all these explorations, C was found to prevail over P, qualitatively in the same way as in Fig. 4(a).

IV. DISCUSSION

Within the molecular field theory of thermotropic biaxial nematic liquid crystals governed by the generalized quadrupolar potential of mean torque in Eq. (2), we have computed the ratio ρ of the biaxial-to-uniaxial and uniaxial-to-isotropic transition temperatures. We found that ρ is almost independent of the parameter γ, and we interpreted this as a quantitative indication that the term in λ is the dominant biaxial interaction. However, a close comparison between this theory and the experimental data for the order parameters of tetrapode A in [8] showed a degree of disagreement.

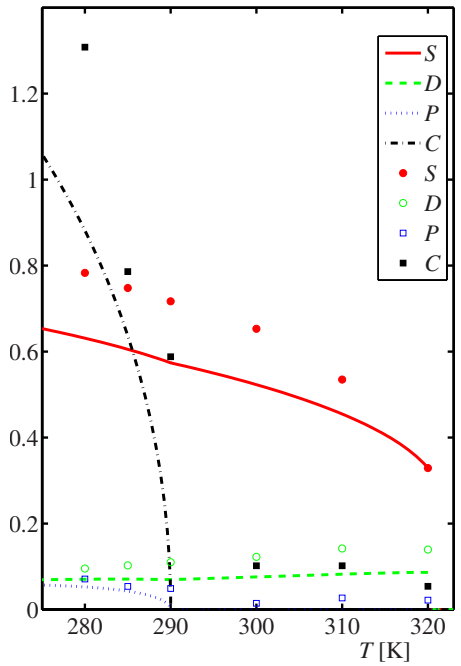

FIG. 5. (Color online) Order parameters (S,D,P,C) obtained in [28] for biaxial GB particles compared with the predictions of the theory based on the generalized quadrupolar potential of mean torque in Eq. (2). The point characterizing this biaxial GB interaction on the (γ,λ) plane occurs for $\gamma=\gamma_{GB}=0.134$ and $\lambda=\lambda_{GB}=0.172$; it lies along the isoratio line for $\rho=\rho_{GB}=0.906$. Here the temperature has been scaled arbitrarily so as to place the nematic-to-isotropic transition at $T=320$ K as in Fig. 4. In this temperature scale, the smectic-to-biaxial transition observed in [28] would occur at $T=275$ K. The color code is the same as in Fig. 4, and simulation data are represented through different symbols according to the legend.

Different reasons could explain such a disagreement, among which are the theoretical techniques and model employed to extract the order parameter profiles from the primary experimental data. Indeed the determination of the primary data in [8] is in itself a remarkable achievement, still unequaled in other experimental explorations of thermotropic biaxial nematics. Of course, another reason for the disagreement could rest with the theory; however we do not believe that this is the case. First, the generalized quadrupolar potential of mean torque developed in the theory is completely consistent with that obtained from a variational analysis using the four second-rank orientational order parameters and excluding higher-rank order parameters. Thus, although fourth-rank tensors could be included in the potential of mean torque, it seems unlikely that they would have any significant influence on the general behavior of the predicted order parameters. Second, computer simulations of a relatively realistic model of biaxial particles based on an extension of the Gay-Berne (GB) potential [28] have produced orientational order parameters in good qualitative agreement with the molecular-field theory. In Fig. 5 we compare the

data obtained in [28] for biaxial GB particles with the predictions of the theory illustrated here.[3] Again, the parameters γ_{GB} and λ_{GB} describing the biaxial GB interaction through the generalized quadrupolar potential of mean torque in Eq. (2) were determined by locating along the isoratio line for $\rho_{GB}=0.906$, the point corresponding to the value of S for the uniaxial-to-isotropic transition, $S_{N_U\text{-}I}=0.33$, reported in [28]. Thus, the minor order parameters D and P are indeed small and weakly temperature dependent, whereas the major order parameters S and C are both found to be large and to vary significantly with temperature.

At present, we are not in a position to resolve the apparent inconsistency between theory and experiment described in Sec. III; however, we believe that this problem certainly merits further consideration at both theoretical and experimental levels.

[3] As also recalled in [15], the scalar order parameters employed in [28] are denoted by $\langle R^2_{00}\rangle$, $\langle R^2_{02}\rangle$, $\langle R^2_{20}\rangle$, and $\langle R^2_{22}\rangle$. They are related to S, D, P, and C through the relations $S=\langle R^2_{00}\rangle$, $D=\sqrt{6}\langle R^2_{02}\rangle$, $P=\sqrt{6}\langle R^2_{20}\rangle$, and $C=6\langle R^2_{22}\rangle$.

ACKNOWLEDGMENTS

Financial support from the Royal Society of London through the Project Biaxial Liquid Crystals: Mathematical Models and Simulation and from the Leverhulme Trust (G.R.L.) are gratefully acknowledged.

[1] M. J. Freiser, Phys. Rev. Lett. **24**, 1041 (1970).
[2] M. J. Freiser, Mol. Cryst. Liq. Cryst. **14**, 165 (1971).
[3] G. R. Luckhurst, British Liquid Crystal Society Newsletter, August, 10 (2005). See http://www-g.eng.cam.ac.uk/blcs/
[4] S. Kumar, Patent Application WO 2007/025111 A1.
[5] G. R. Luckhurst, Thin Solid Films **393**, 40 (2001).
[6] L. A. Madsen, T. J. Dingemans, M. Nakata, and E. T. Samulski, Phys. Rev. Lett. **92**, 145505 (2004).
[7] B. R. Acharya, A. Primak, and S. Kumar, Phys. Rev. Lett. **92**, 145506 (2004).
[8] K. Merkel, A. Kocot, J. K. Vij, R. Korlacki, G. H. Mehl, and T. Meyer, Phys. Rev. Lett. **93**, 237801 (2004).
[9] J. L. Figueirinhas, C. Cruz, D. Filip, G. Feio, A. C. Ribeiro, Y. Frere, T. Meyer, and G. H. Mehl, Phys. Rev. Lett. **94**, 107802 (2005).
[10] K. Neupane, S. W. Kang, S. Sharma, D. Carney, T. Meyer, G. H. Mehl, D. W. Allender, S. Kumar, and S. Sprunt, Phys. Rev. Lett. **97**, 207802 (2006).
[11] P. G. de Gennes and J. Prost, *The Physics of Liquid Crystals* (Oxford University Press, Oxford, 1993). See Sec. 2.1.1.3.
[12] D. A. Dunmur and K. Toriyama, in *Physical Properties of Liquid Crystals*, edited by D. Demus, J. Goodby, G. W. Gray, H.-W. Spiess, and V. Vill (Wiley-VHC, Weinheim, Germany, 1999), Chap. IV, Sec. I.
[13] D. A. Dunmur and K. Toriyama, in *Handbook of Liquid Crystals*, edited by D. Demus, J. Goodby, G. W. Gray, H.-W. Spiess, and V. Vill (Wiley-VCH, Weinheim, Germany, 2001), Chap. VII, Vol. 1A, p. 189.
[14] A. M. Sonnet, E. G. Virga, and G. E. Durand, Phys. Rev. E **67**, 061701 (2003).
[15] R. Rosso, Liq. Cryst. **34**, 737 (2007).
[16] J. P. Straley, Phys. Rev. A **10**, 1881 (1974).
[17] G. De Matteis and E. G. Virga, Phys. Rev. E **71**, 061703 (2005).
[18] G. De Matteis, S. Romano, and E. G. Virga, Phys. Rev. E **72**, 041706 (2005).
[19] F. Bisi, E. G. Virga, E. C. Gartland, Jr., G. De Matteis, A. M. Sonnet, and G. E. Durand, Phys. Rev. E **73**, 051709 (2006).
[20] G. De Matteis, F. Bisi, and E. G. Virga, Continuum Mech. Thermodyn. **19**, 1 (2007).
[21] W. Maier and A. Saupe, Z. Naturforsch. A **14**, 882 (1959). Translated into English in T. J. Sluckin, D. A. Dunmur, and H. Stegemeyer, *Crystals that Flow*, pp. 381–385. (Taylor & Francis, London, 2004).
[22] L. Longa, P. Grzybowski, S. Romano, and E. Virga, Phys. Rev. E **71**, 051714 (2005).
[23] F. Bisi, S. Romano, and E. G. Virga, Phys. Rev. E **75**, 041705 (2007).
[24] See http://www.matcont.ugent.be/matcont.html
[25] MATLAB is a registered trademark of The MathWorks, Inc., http://www.mathworks.com
[26] F. Bisi, E. C. Gartland, Jr., and E. G. Virga (unpublished).
[27] G. De Matteis, A. M. Sonnet, and E. G. Virga (unpublished).
[28] R. Berardi and C. Zannoni, J. Chem. Phys. **113**, 5971 (2000).
[29] M. Kröger, A. Ammar, and F. Chinesta, J. Non-Newtonian Fluid Mech. **149**, 40 (2008).